NASA CR 66677

COMPOSITE SOLID PROPELLANT FLAME MICROSTRUCTURE DETERMINATION

By Dr. Raymond Friedman, Dr. Martin Hertzberg,
Dr. Edward T. McHale, Dr. Guenther von Elbe

Prepared under Contract No. NAS1-7457 by

Kinetics and Combustion Group
Atlantic Research Corporation
A Division of The Susquehanna Corporation
Shirley Highway at Edsall Road
Alexandria, Virginia 22314

for

NATIONAL AERONAUTICS AND SPACE ADMINISTRATION

ANNUAL REPORT

June 23, 1967 - June 22, 1968

COMPOSITE SOLID PROPELLANT FLAME MICROSTRUCTURE DETERMINATION

Contract No. NAS1-7457

To:

National Aeronautics and Space Administration
Langley Research Center
Langley Station
Hampton, Virginia 23365

Project Directors: Dr. R. Friedman
Dr. G. von Elbe

Project Scientists: Dr. M. Hertzberg
Dr. E. T. McHale

Kinetics and Combustion Group
Atlantic Research Corporation
A Division of The Susquehanna Corporation
Alexandria, Virginia

ABSTRACT

The objectives of this study are (1) the development of an experimental capability to probe the structure of heterogeneous propellant flames and (2) the utilization of this capability for exploration of the various contiguous flame zones. The purpose is an improved understanding of propellant flame characteristics by acquisition of definitive data on the physical and chemical processes in the combustion zone.

The flame structure is composed of the interdependent fields of temperature, mass flow and distribution of molecular species. It is not possible to miniaturize the required probes to the extremely small scale required by flames in an ordinary combustion environment. However, at low pressures the scale becomes sufficiently large to accommodate technically feasible microprobes, and it also appears feasible on the basis of existing theory to scale a flame structure that is mapped at low pressure to the length and time dimensions of flames in a high-pressure environment.

On this basis probes have been developed for low-pressure flames of pressed strands of ammonium perchlorate (AP) and combinations of AP strands with sheets of organic binders in sandwich configurations. The temperature is measured by fine thermocouples embedded in the sample. The gas flow is observed by the particle track method. The distribution of molecular species is determined by means of small stationary or moving sampling probes leading to a mass spectrometer. The combustion chamber contains windows for visual and motion-picture observation of burning propellant specimens and is fitted with various mounts and connections for inserting the sampling probe, admitting inert gas and maintaining the desired pressure. It also contains a germanium window to allow a laser beam to enter the chamber. The laser beam provides a precisely controllable auxiliary heat flux to the surface of the burning AP or AP-binder sample. This arrangement makes it possible to maintain a flame in low-pressure

regimes where the heat feed-back from the flame gas to the sample material is insufficient for flame propagation.

In experiments with pressed AP strands the control of the laser radiation flux was utilized to determine the effect of flux on the burning rate, i.e., the rate of regression of the AP-surface, and to determine the threshold flux required for ignition. Most of these experiments were performed at atmospheric pressure but some data were also obtained at low pressures down to 36 torr. The threshold flux for ignition in cals $cm^{-2}sec^{-1}$ was found to increase with decreasing pressure from 2.8 cals cm^{-2} sec^{-1} at 760 torr to more than 28 cals cm^{-2} sec^{-1} at 36 torr. It is known that AP does not burn below 22 atmospheres without an auxiliary heat flux. The threshold burning rate at 22 atmospheres is 0.25 cm sec^{-1} and the corresponding heat flux is estimated to be 130 cals cm^{-2} sec^{-1}. For laser-supported burning at a pressure of one atmosphere the flux corresponding to this burning rate was found to be 120 cals cm^{-2} sec^{-1}.

Mass-spectroscopic sampling was performed with pure AP-flames and AP-binder sandwich flames. Composition traverses of the latter flames have yielded excellent definition of the regions of fuel-oxidizer burning and pure AP burning. AP-flames contain substantial amounts of oxides of nitrogen; they consist principally of NO but N_2O and NO_2 are also present. A significant intermediate product found in the zone of fuel-oxidizer combustion is C_2H_2.

The thermocouple probes have yielded temperature profiles of high quality. The observed pressure-dependent surface temperatures of AP, ranging from 690° to 780°K, are in excellent agreement with measurements of previous investigators. The observed flame temperatures of 1900° to 2000°K are intermediate between the temperature of pure AP ($\sim$1200°K) and of a propellant mixture ($\sim$2700°K), as is expected for diffusion flames of this type.

The visualization of flow lines and measurement of mass velocities differs from previous investigations of this kind on gas flames, inasmuch as the tracer particles are initially at rest at the interface between flame

gas and solid propellant and are therefore subjected to much larger acceleration than in the case of particles moving with the stream through the combustion zone of a gaseous fuel-oxidant mixture. It is therefore necessary to interpret the observed particle tracks in terms of drag force and momentum increase. This problem has been investigated and the capability of mapping the flow field within acceptable limits of accuracy has been demonstrated. Data are at present scanty but they provide sufficient leads toward methods for improving the quality and quantity of track observations to justify confidence in the experimental capability for this phase of flame probing.

Future work is expected to implement the objectives of the program by acquisition of systematic data on temperature, flow and molecular species distribution that permit the mapping of low-pressure flame structures and serve the purpose of an improved understanding of propellant flame characteristics.

TABLE OF CONTENTS

I. INTRODUCTION

This report describes the development of experimental apparatus and techniques for investigating the detailed structure of heterogeneous propellant flames. The task to be performed comprises the development of probes and probing techniques to monitor the three structural elements of the flame, namely, the temperature field, the field of interdiffusion and chemical reaction of the fuel and oxidizer components, and the aerodynamic flow pattern. It is generally agreed that in the absence of an experimental capability of this type little further progress can be expected in the scientific understanding of propellant combustion, but hitherto the problem has largely been regarded as not amenable to a practical solution. This is due to the fact that in an ordinary combustion environment it would be necessary to probe the field dimensions and field changes on a length and time scale of the order of microns and microseconds; and it is readily apparent that no existing method of monitoring events on such small scale is applicable to the present problem. It is therefore necessary to consider whether a combustion environment can be established in which the length and time scale is sufficiently large to accommodate technically feasible microprobes, and whether data obtained on this expanded scale have meaningful relations to ordinary combustion environments.

In developing the concept of the present program the latter question has not been considered to be a serious obstacle. In particular, if a flame structure is mapped out at low pressure, it should not be prohibitively difficult to scale the flame to a high-pressure environment. One would apply existing knowledge to the effect of pressure on the chemical and physical parameters that determine the flame structure; and although the problem is complicated by the interdependence of the fields of temperature, molecular-species distribution and flow,it is not unmanageable.

On this basis the decision has been made to use low-pressure flames of ammonium perchlorate and organic binder material. The oxidizer and fuel are combined as parallel slabs in sandwich configuration and burned

at pressures between 1 - 760 torr. A laser source is used to provide flame-supporting heat flux at low pressure where the heat feed-back from the flame is not sufficient to maintain the flow of pyrolysis gas from the solid material into the flame zone. The experimental apparatus and procedures permit variation of the ambient pressure, the radiant flux, the thickness of the polymer slab in the sandwich configuration, the chemical type of the polymer, and other parameters. The techniques for probing the fields of temperature, chemical composition and flow comprise fine thermocouples and optical pyrometry, capillary probe sampling into a mass spectrometer, and particle tracks for flow observation.

Some of these probing techniques are novel and hence a considerable experimental effort had been necessary to establish their feasibility and practical application. Other techniques have been used previously in similar experimental work. The present program, however, exceeds the scope of previous work inasmuch as it envisages an integral system of probing techniques for exploring the structure of solid-propellant flames. As will be seen from the material presented below, this objective has been substantially accomplished. Using the demonstrated experimental capability it is now possible to expand the research objective to systematic data acquisition that will permit an understanding of the various combustion zones and the physical and chemical processes which occur within these distinct zones. The continuation of the program along these lines may be expected to yield additionally an increased technical experience and refinements of observational procedures that should benefit the efficiency and accuracy of data acquisition.

II. EXPERIMENTAL APPARATUS AND TECHNIQUES

A. SAMPLE PREPARATION

Sandwich-type samples were used in this study which consisted of two slabs of compacted ammonium perchlorate (AP), one on either side of a thin layer of polymer. These sandwiches represent an idealized composite solid propellant configuration which lend themselves to micro-probing. The polymer was generally 0.5 mm thick except for the composition measurements in which the polymer was 1.5 mm thick. It usually consisted of polymethylmethacrylate (PMM). Sketches of samples are shown in Figures 10 and 11. The AP was compacted from 200μ powder into strands of 4 x 4 x 38 mm in size and of ~95 percent of crystal density. The mold used for the pressing is described in reference 1.

Most sandwiches were prepared by slipping the polymer, cut to size, into the center of the loose AP in the mold and pressing the sandwich in one operation. For temperature or flow measurements, samples were made by glueing the AP slabs to the polymer and inserting a thermocouple or particles into the glued surface (Figure 9). The glue consisted of PMM dissolved in some organic solvent. Samples consisting of two 2 mm thick pieces of AP on a 0.5 mm piece of PMM represent a very oxidizer-rich system (overall), the oxidizer to fuel ratio being about 5 to 1.

In some of the future experiments, at the sponsor's direction, it is planned to use sandwiches made from single crystals of AP. In the course of the program we have obtained a quantity of these crystals of various sizes from Dr. H. C. Beachell of the University of Delaware.

B. TEMPERATURE PROBE

The thermal structure of the deflagration wave of the sandwich propellants was determined by embedding fine thermocouples in the samples. Pt-Pt/10% Rh thermocouples with bead diameters of approximately 125μ were used. These melt at 2045°K (they will withstand somewhat higher gas temperatures because of radiant cooling) and were found to survive in the sandwich flames at 0.1 atm pressure at low radiant fluxes. A complete mapping of the

temperature field requires that the profiles be determined at points through the AP, the binder, and at the AP-binder interface. Only the last type of profile was measured to date in the program. Incorporating the thermocouple into the sandwich was accomplished by placing the bead on the polymer strip and cementing in place with PMM glue. The sandwich was then prepared by glueing the two slabs of AP in place. The leads were then mounted on holders in the combustion chamber in such a way that the thermocouple did not move out of the binder-interface plane when the bead emerged from the solid sandwich into flame gas during the combustion. The thermocouple output was recorded with a Visicorder. Its position during the combustion could be determined from motion pictures.

C. AERODYNAMIC MEASUREMENTS

The gas flow pattern and velocity through the flame comprise essential parts of the flame structure. The approach taken to determine these was to incorporate fine particles into the sandwich and photograph the particle tracks during combustion under high-intensity illumination. A slurry of aluminum oxide particles (of various sizes but usually 5 , see III-B-2) in a solvent was prepared and these were painted onto the polymer slab in a very fine line along the length (see Figure 9). The sandwich was then glued together. During the burning, the system was illuminated with a flashbulb, using slits and reflectors as required (references 2, 3). Particle tracks were photographed at right angle to the lighting with a 16 mm motion picture camera.

Further improvements in the particle track measuring technique are anticipated. These include use of lenses, a still camera, electronic flash unit, and interrupting sector disc.

D. COMBUSTION CHAMBER

The reactor consists of a stainless steel cylinder 7 inches high by 6 inches in diameter. The top and bottom are closed by 6-inch plates on flanges. The top plate contains a mount through which the quartz microprobe enters the chamber. It also provides a window through which the particles can be illuminated for flow pattern measurements. Four and one-half inch flange openings are provided in the front and rear of the chamber. The front opening is closed by a 1/2" thick disc of quartz which allows visual observations and motion pictures to be taken. The rear opening contains fittings to admit inert gas and also to connect to a high-capacity (20 liter sec^{-1}) Stokes vacuum pump and manometers. (see Figure 2).

On both sides of the chamber there are 2-1/2" flange openings. The one contains a germanium window to allow the laser beam to enter the chamber. The other has a graphite block attached to it to absorb and dissipate laser energy. Inside the reactor there are two electrical posts to take thermocouple leads and one other support to hold the sandwich propellant. The sample is held in place with a spring clip attached to the support.

E. RADIANT LASER SOURCE

The external radiant heat source used to sustain the low-pressure combustion processes consisted of a Model 40, CO_2 Gas Laser. The output wavelength is 10.6μ; the nominal output power, 100 watts; the nominal beam diameter 1.5 cm. The instrument was purchased from the Coherent Radiation Laboratories, Palo Alto, California.

The output power and intensity distribution were measured with a Model 201 Power Meter obtained from the same manufacturer. The results of these measurements are shown in Figure 1. The unfocused beam readily provides radiant energy fluxes in the range 0 - 30 cal/cm^2 sec. These intensities were generally sufficient to sustain the combustion processes at atmospheric and sub-atmospheric pressures. The total power output, as shown in (a), is a monotonically increasing function of the tube current. The beam initially converges from the output mirror to some minimum diameter

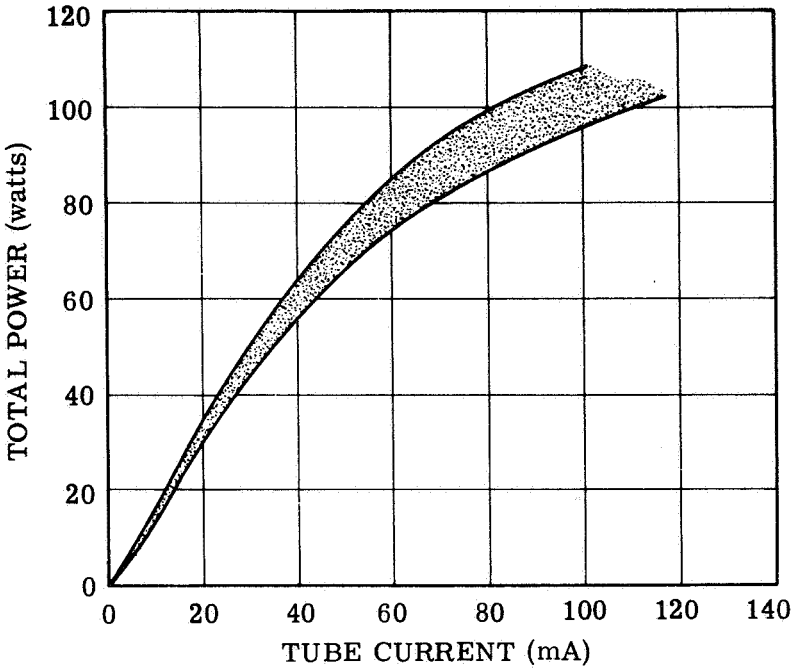

a. Total Power Versus Tube Current (13 torr Tube Pressure, Tuned to Peak Power)

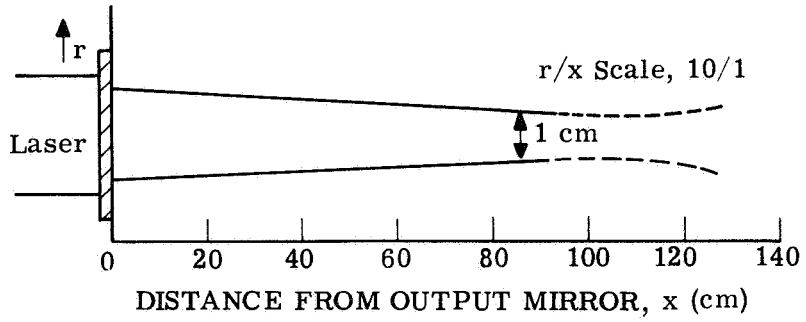

b. Beam Divergence (Unfocused) Tube Current: 50 mA

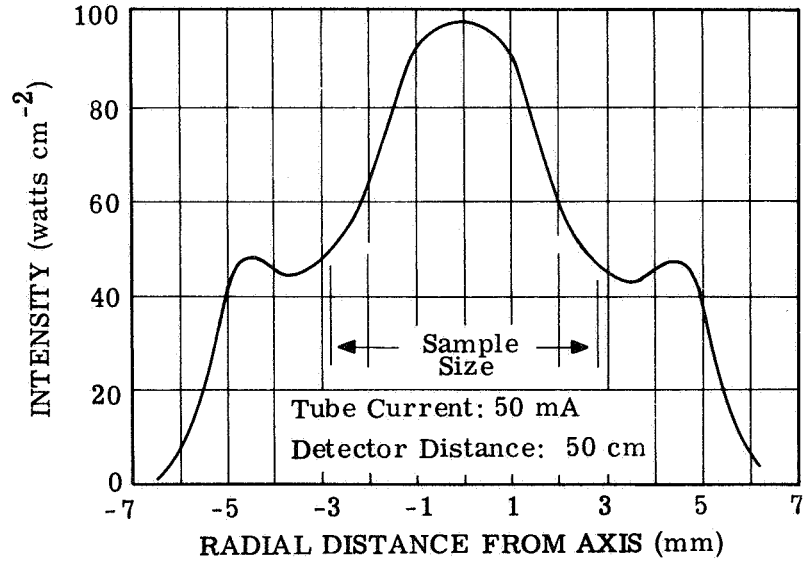

c. Radial Intensity Distribution

Figure 1. Laser Output Power and Intensity Distribution.

at a distance of at least one meter from the output reflector, and then diverges again as shown in (b). The convergence angle is apparently a function of the output power. It is caused by a radial temperature gradient in the output reflector which causes it to act as a slightly convergent lens. The radial intensity distribution is depicted in (c). As can be seen, the intensity distribution varies across an aligned sample, with the intensity at the center of the sample almost a factor of two higher than the intensity at the sides of the sample. The spatially averaged radiant intensity across the sample is thus approximately 80% of the peak radiant intensity.

In view of this intensity distribution, considerable care was generally taken to align the sample axis along the laser axis. The samples were generally burned at given distance from the output mirror. Inaccuracies in alignment were readily discernible since they caused uneven combustion. Estimates of the inaccuracies introduced by these geometrical variations are of the order of 20%.

The problem of non-uniformity of energy flux in the laser beam is being attacked by other investigators who are also using the CO_2 laser for solid propellant combustion studies, notably the groups at NASA Langley and at Princeton. The former group is attempting to reflect the laser beam off a mirror which is rotating eccentrically at a slight angle to the normal. This technique would, for instance, take a spot of light and reflect it as a circle. The Princeton group is passing the focused beam through a light pipe or kaleidoscope. This scrambles the beam somewhat but the coherent character of the light tends to produce interference patterns which are non-uniform unless the optical system is very carefully aligned. An additional refinement of both techniques would be to incorporate a vibrator into the system. Both methods offer an improvement and we have devoted considerable effort toward refining the light pipe. In addition, we have attempted to scramble the beam by passing it through salt wafers made by compacting NaCl. It was thought that the diffraction and refraction of the light by the crystals might diffuse the beam. Various particle sizes were compacted at several pressures but rather minimal scrambling was obtained even with the

most efficient of these wafers. Another approach which we have tried is passing the beam through a spatial filter. This consists of focusing the light at a pinhole, the size of which is slightly smaller than the so-called "circle of confusion" at the focal point. The pinhole was made in a heavy copper bar and the emerging beam was collimated, but little improvement in flux uniformity was obtained. Finally, a mode-selection aperture, which is supplied by the manufacturer, was tried and this too was of little help. It was found that as good a method as any of destroying the mode patterns of the laser output is to simply misalign the cavity mirrors in the laser head. This does not produce a high degree of uniformity, but it is satisfactory for the present and has resulted in some improvement in producing flatter regressing surfaces on burning sandwiches.

In spite of these uncertainties, the laser source is substantially superior to previous sources for these purposes. These high radiant fluxes are readily obtained in the unfocused beam, whereas arc-image or filament-image source requires focusing in order to obtain comparable intensities. The geometrical uncertainties of focused arc- or filament-image sources are much larger than those of the collimated laser sources. Furthermore, the laser-induced flames are readily visible since the source energy is in the infrared and does not generate interfering background luminosity.

F. COMPOSITION PROBE

The composition measurements were obtained with the apparatus depicted in Figure 2. The apparatus consists of the high-power laser source, a combustion chamber, a mass spectrometer sampling system and the associated vacuum and high vacuum pumps. Radiant power from the laser source passed through a germanium window and impinged upon the sample. The samples were generally burned in inert atmospheres ranging from 3 - 760 torr. The combustion products were sampled with a quartz sampling probe leading to a mass spectrometer. The combined heat from the laser and the sample flame would easily melt probe tips made of Pyrex glass; however, quartz probes of sufficient wall thickness generally performed satisfactorily. The probes aperture was of the order of 0.01 mm in diameter at the probe tip, and tapered out conically to diameter of 2-3 mm at distances of 10 cm above the sample.

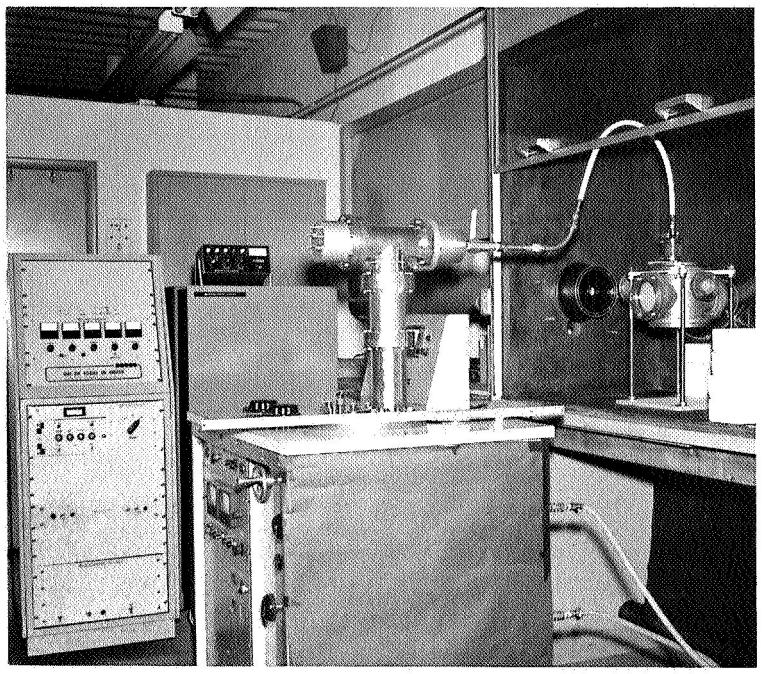

Solid Propellant
Microstructure Laboratory

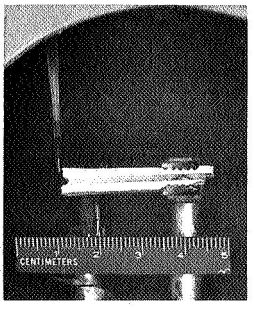

Composite Sample
with Quartz Probe

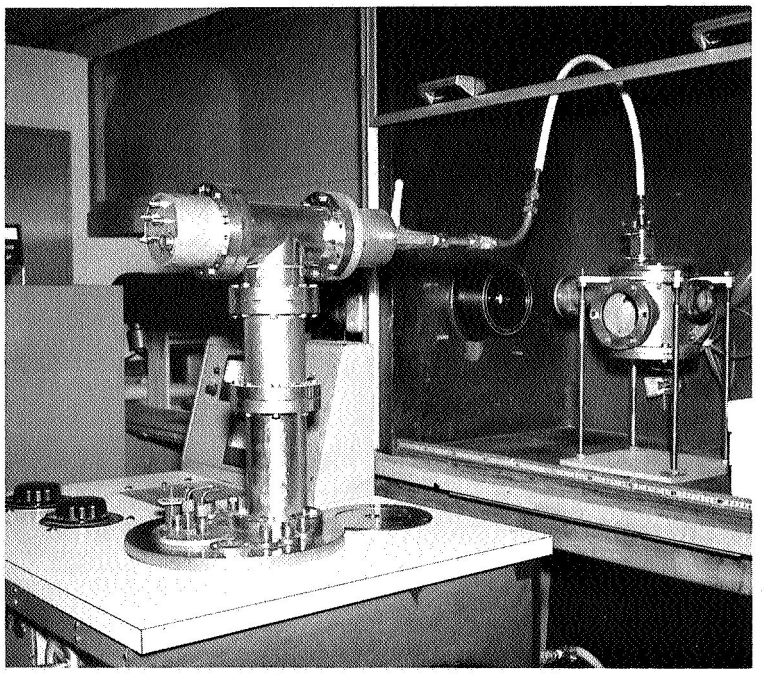

Laser Beam Output, Combustion
Chamber and Mass Spectrometer

19621

Figure 2a. Experimental Apparatus.

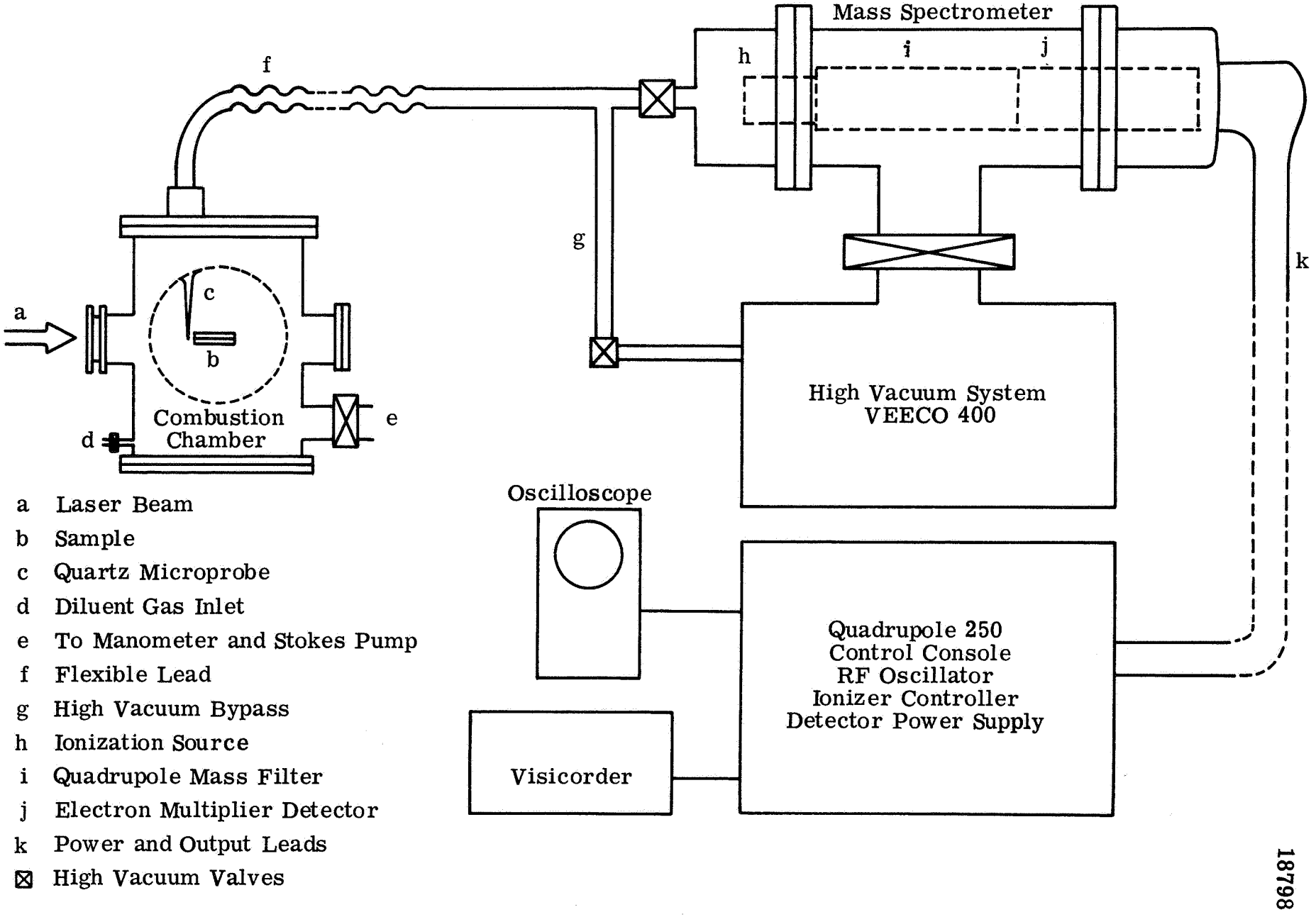

Figure 2b. Composition Probe Apparatus.

The sampled combustion products were analyzed with a Quad 250 Residual Gas Analyzer purchased from the Ultek Corporation, Palo Alto, California. The source was a type 353 axial beam ionizer; the detector a conventional electron-multiplier. The spectrometer was initially isolated from the probe and evacuated to pressures of the order of 10^{-7} torr with a Veeco 400 high vacuum system. The sampled combustion products were then passed through the spectrometer until a background pressure of the order of 10^{-5} torr was obtained. A complete spectrum of the combustion products was obtained every 0.2 to 0.4 seconds. The observed spectra were displayed on an oscilloscope, where they could be photographed; or alternatively, the output signal was fed to a recorder.

The mass spectrometer can be operated in three mass ranges: 1 - 50, 10 - 150, and 50 - 500 AMU. Generally,the lowest mass range was sufficient to identify the combustion products. The instrument has performed very satisfactorily from the time of its initial purchase and installation. Several problems were encountered and were readily resolved. The frequency response of the output system was not rapid enough to follow the peak shapes at sweep times faster than 0.2 seconds per sweep. This situation was improved somewhat by using a special low-capacitance output cable. A solution to the problem of rapid-scan data recording has been demonstrated: it involves the use of an emitter-follower output amplifier, coupled to a recording oscilloscope. Complete spectra were thus obtainable in sweep times of 0.01 seconds per spectrum. This was not a serious problem, since for all steady-state experiments sweep times of the order of 0.2 seconds were satisfactory. However, faster scan capability is desirable for ignition and transient studies.

Preliminary measurements of the transmission factor of the instrument were made in the low, medium, and high mass ranges by using known mixtures of rare gases. The results indicate essentially little or no mass discrimination effects when the instrument is operating in the low mass range at resolving powers of 50 or less. There is, however, appreciable mass discrimination at higher resolving powers. For example, for 1 AMU resolution at mass 130, in the high mass range, the transmission factor for the

heavier masses was of the order of 1/3 of the transmission factor for the lighter masses (where $m/\Delta m < 50$).

Several sampling systems were fabricated and tested. The major problems were: (1) the design of a probe tip which was small enough and delicate enough not to disturb the flame, but rugged enough to withstand the combined heat flux from the flame and the laser; and (2) the design of a sampling tube which minimizes the sampling time-constant and also minimizes the absorption of species on the wall. Problem (1) was resolved by using a tapered, thick-wall, quartz microprobe which was able to withstand the heat flux although it would glow red-hot in the sample flame. In order to solve problem (2), the sampling tube was made of as large-diameter flexible line as possible. A flexible stainless-steel line initially used was found to be a strong source of H_2O (and HCl) absorption. It was replaced by a flexible teflon sampling tube. Sampling time constants are presently in the hundreds of milliseconds range, and this appears to be satisfactory for the 0.2 second scan times.

III. RESULTS AND DISCUSSION

A. PURE AMMONIUM PERCHLORATE

1. Flame Characteristics

The monopropellant flame above pure AP is representative of the initial structure of the composite flames for perchlorate propellants, and is therefore a zero order approximation of the propellant diffusion-flame. Furthermore, the pure AP flame controls the composite burning rate at high pressures.[8] Accordingly, the initial experiments were performed with the pure monopropellant.

The flow pattern observed when pure AP was burned in the laser beam was generally laminar. The flux-induced flame is a stable orange flame that was readily observed and photographed. Photographic records of the flame structure for a wide variety of pressures and radiant fluxes have been compiled.

2. Burning Rate and Ignition Delay vs. Radiant Flux

The non-adiabatic burning rate for pressed powders of pure AP in air, at one atmosphere, was measured as a function of incident flux intensity. The results of these measurements are shown in Figure 3. The data points represent many individual experimental runs. The total scatter for all runs is large, however the rate data during any given run were quite linear functions of the source power. The spread in the data points was caused by several factors: errors in measuring the total source power, errors in determining the spatial distribution of the source intensity, random variations in the intensity distribution, and inaccuracies in the sample alignment.

The measured ignition threshold at 2.8 cals cm^{-2} sec^{-1} is the minimum intensity required to ignite the surface with a clearly visible flame. Above this threshold the sample burns readily with a visible flame, while below this threshold, the sample slowly sublimes (recondensing on the cold surroundings).

It is reasonable to assume that the observed induction time at the ignition threshold is approximately equal to the time required to reach steady-state equilibrium. A steady state energy balance at this threshold gives:

$$\dot{x}_o \left\{ \rho_x \left[(C_g)_g T_b - (C_g)_x T_u + \Delta H_g \right] + i(T,\alpha,\lambda) \right\} + (I_L)_o = -(I_R)_o \Big|_{\text{at threshold}} \qquad (1)$$

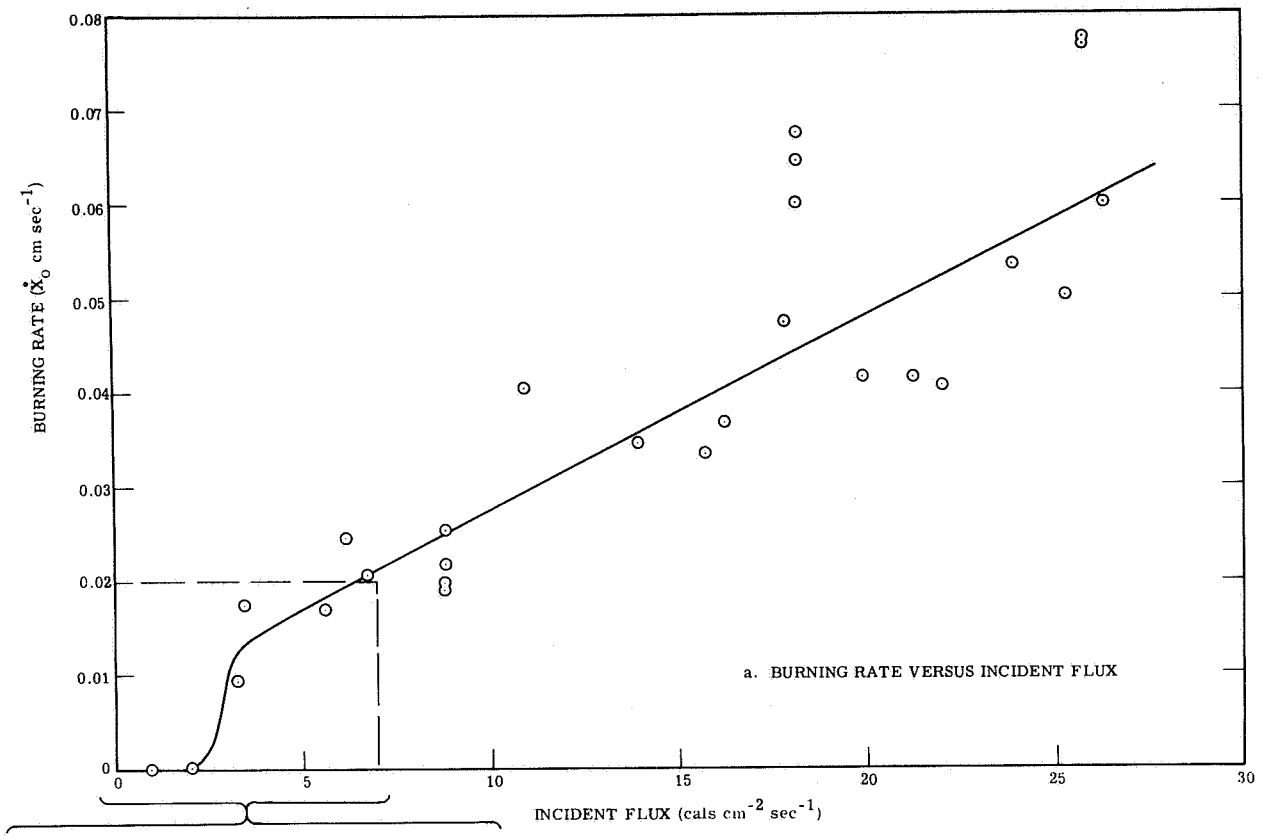

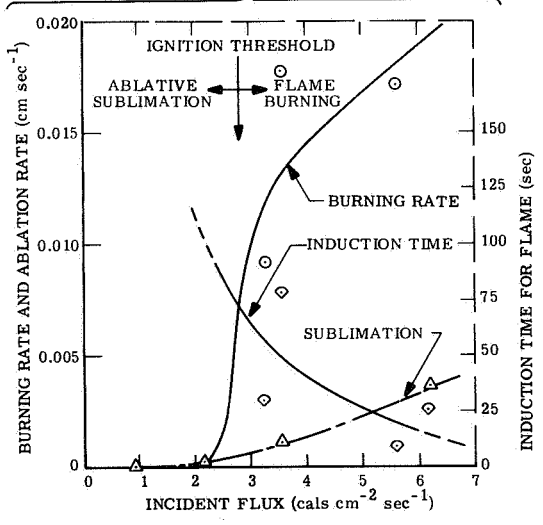

b. INDUCTION TIME, BURNING RATE AND SUBLIMATION RATE VERSUS INCIDENT FLUX NEAR IGNITION THRESHOLD.

Figure 3. Laser-Induced Combustion of Ammonium Perchlorate (In Air at One Atmosphere, Laser Wave Length is 10.6 μ).

The symbols used in this and the subsequent equation are defined in Section VI. The net radiant intensity is the difference between the incident flux and the sum of reflected and re-radiated fluxes:

$$-(I_R)_o = (1 - r)\, I - \varepsilon_s \sigma \bar{T}_s^4 \Big|_{\text{at threshold}} \tag{2}$$

The absorbed fraction of the incident energy is (1 - r)I. The fraction $\varepsilon_s \sigma \bar{T}_s^4$ is re-radiated to the surroundings. The remainder is absorbed as latent heat, as sensible heat, or is lost to the surroundings by conductive-convective processes. The maximum re-radiated loss for an assumed surface temperature of 830°K is 0.65 cals cm^{-2} sec^{-1}. This estimate is probably somewhat higher than the real loss at the ignition threshold. The energy absorbed as latent heat just below the ignition threshold is 0.71 cals cm^{-2} sec^{-1}. The sensible heat term is difficult to estimate because the quantity $(C_g)_g\, T_b$ is not known accurately; however, a reasonable estimate is of the order of 0.4 cals cm^{-2} sec^{-1}. The remaining 1.0 cals cm^{-2} sec^{-1} is thus the sum of reflectance and conductive-convective losses. It is further assumed that at these low burning rates $\dot{x}_o\, i(T,\alpha,\lambda) << (I_L)_o$. These estimates of non-adiabatic losses, together with previously reported data for the other parameters, may now be substituted into the equation:[4]

$$\dot{x}_o = \frac{v_{A\to B}\, \rho_g[(C_g)_B T_b - (C_g)_A T_p] - (I_R)_o - (I_L)_o}{\rho_x[(C_g)_g T_b - (C_g)_x T_u + \Delta H_g] + i\,(T,\alpha,\lambda)} \tag{3}$$

Below the ignition threshold $v_{A\to B} = 0$, and one observes only ablative sublimation in the presence of the laser source. The fair agreement between the observed and calculated energy fluxes below threshold indicates that equation 3 predicts the sublimation rate fairly well. Above the ignition threshold, $v_{A\to B}$ is finite, and using an estimate of 110 cm sec^{-1} for $v_{A\to B}$, one

obtains:

$$\dot{x}_o = [\ 6._0 + 0.8\ I\ (\text{cals cm}^{-2}\ \text{sec}^{-1})\ ] \times 10^{-3}\ \text{cm sec}^{-1} \qquad (4)$$

The experimental data are compared with the predicted rate in Figure 4. The agreement in absolute magnitude between the predicted and observed rates near threshold is quite good. This is reflected in a predicted intercept of 6.0×10^{-3} cm sec^{-1} that is almost identical with the observed intercept. The observed slope, however, is significantly higher than the predicted slope.

Nevertheless, a linear extrapolation of the average measured rate to the free-burning threshold value of 0.25 cm sec^{-1} (at 22 atm) indicates that a radiant flux of the order of 120 cals cm^{-2} sec^{-1} would be required to sustain this threshold burning rate at 1 atm. This compares favorably with the calculated value for the simulated flame (at 22 atm): $v_{A\to B}\rho_g[(C_g)_B T_b - (C_g)_A T_p] \simeq$ 130 cals cm^{-2} sec^{-1}.

Any differences are logically attributable to three factors. First, a fraction of the incident flux is reflected by the surface. Secondly, there is additional energy conducted to the surface from the 1 atm flame, which adds to the absorbed radiant energy. These first two factors tend to cancel one another. A third factor involves the convective losses which may be both pressure and burning-rate dependent. These factors may be different for the two cases.

The laser-induced combustion process involves two sources of heat, the laser source and the flame source. This fact could account for the discrepancy between the predicted and observed slopes. It was assumed the magnitude of the flame source is constant independent of laser power level. If, however, one assumes a moderate increase in $v_{A\to B}$ with increasing source power, the predicted slope would show better agreement with the observed data.

3. Burning Rate and Ignition Flux vs. Pressure

Measurements of the pressure dependence of the burning rate are shown in Figures 5 and 6. Although these data are of a preliminary nature, tentative

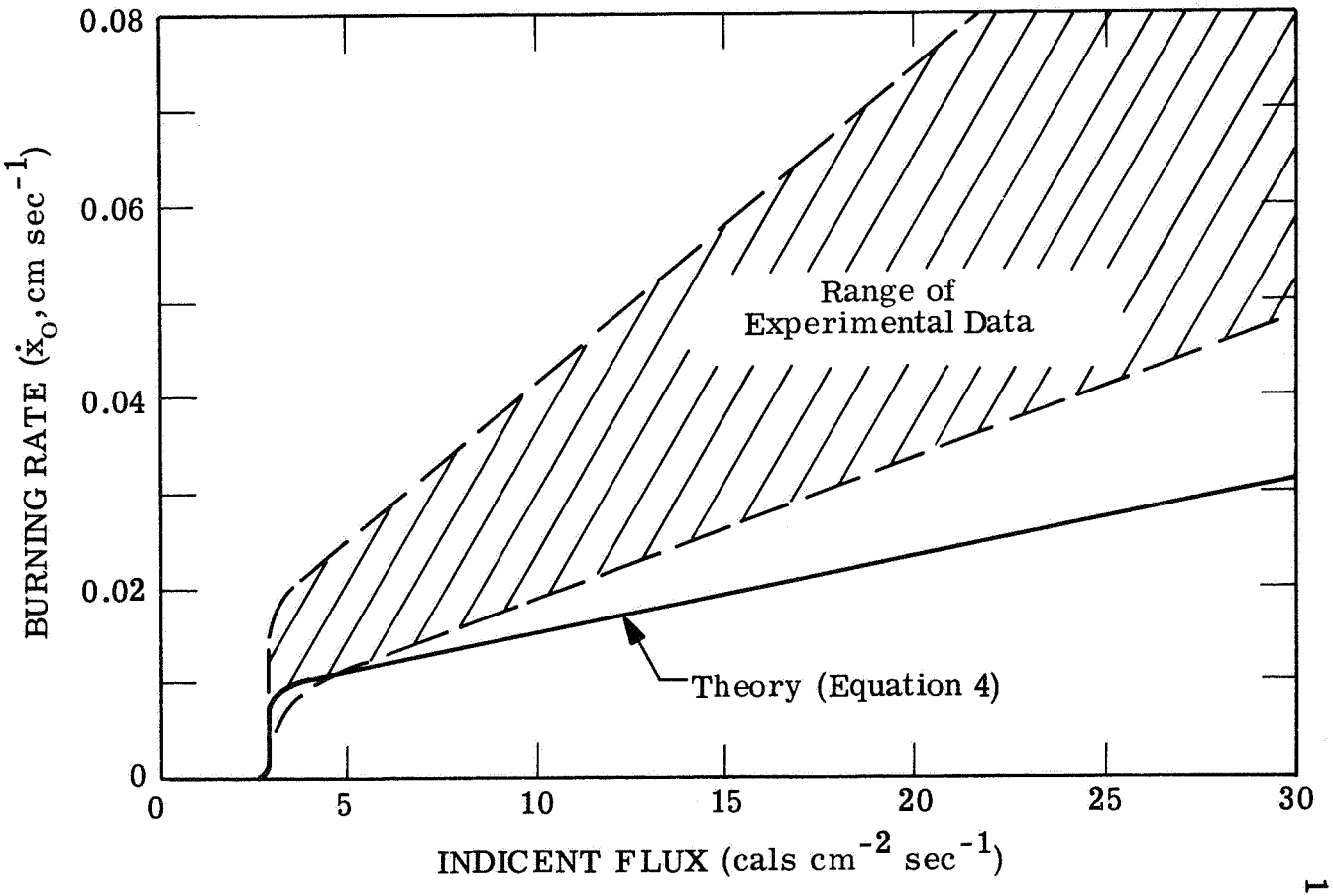

Figure 4. Laser-Induced Combustion of Ammonium Perchlorate, Theory and Experiment.

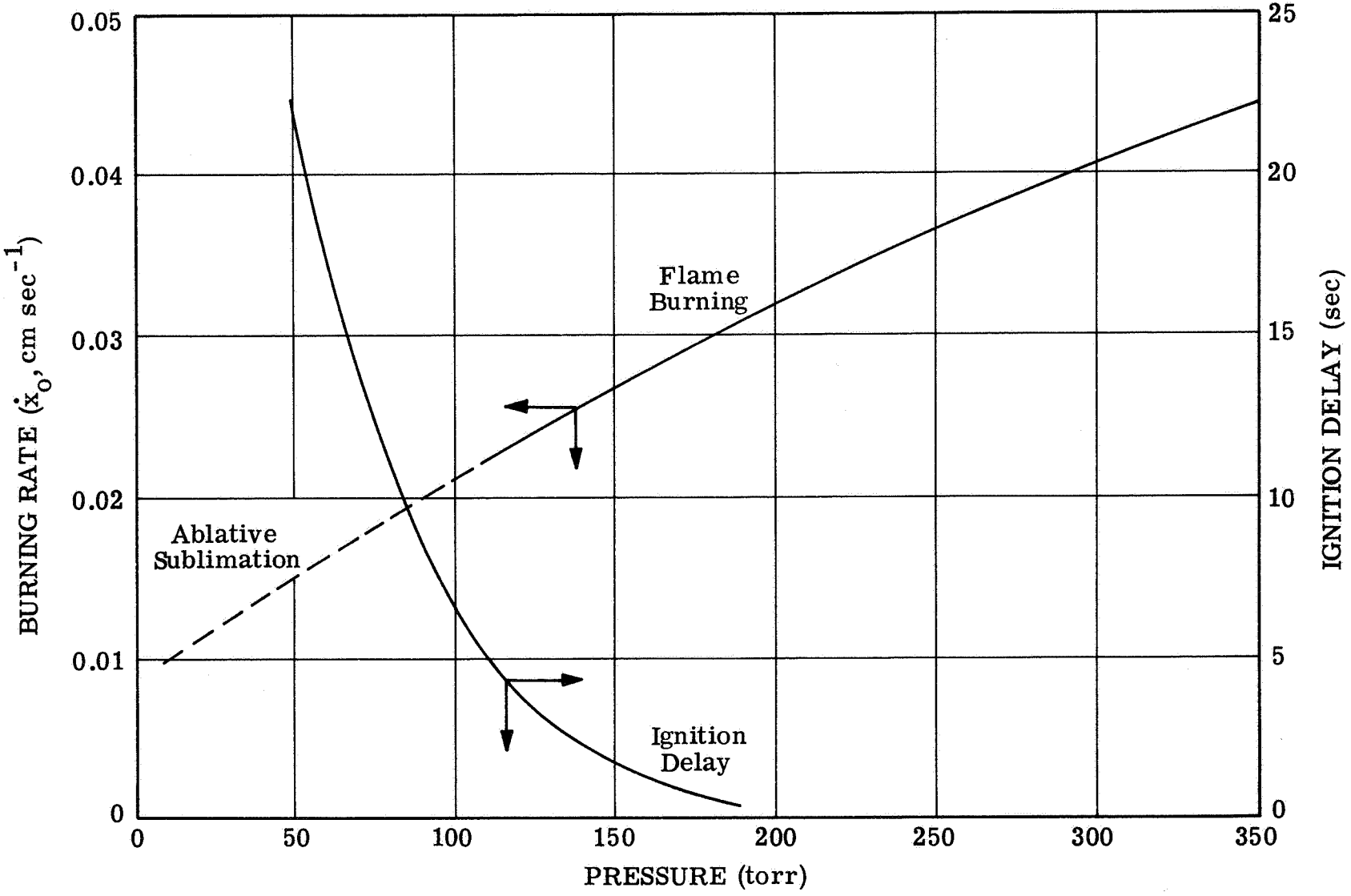

Figure 5. Burning Rate and Ignition Delay Versus Pressure
Constant Radiant Flux: 23 cals cm^{-2} sec^{-1}.

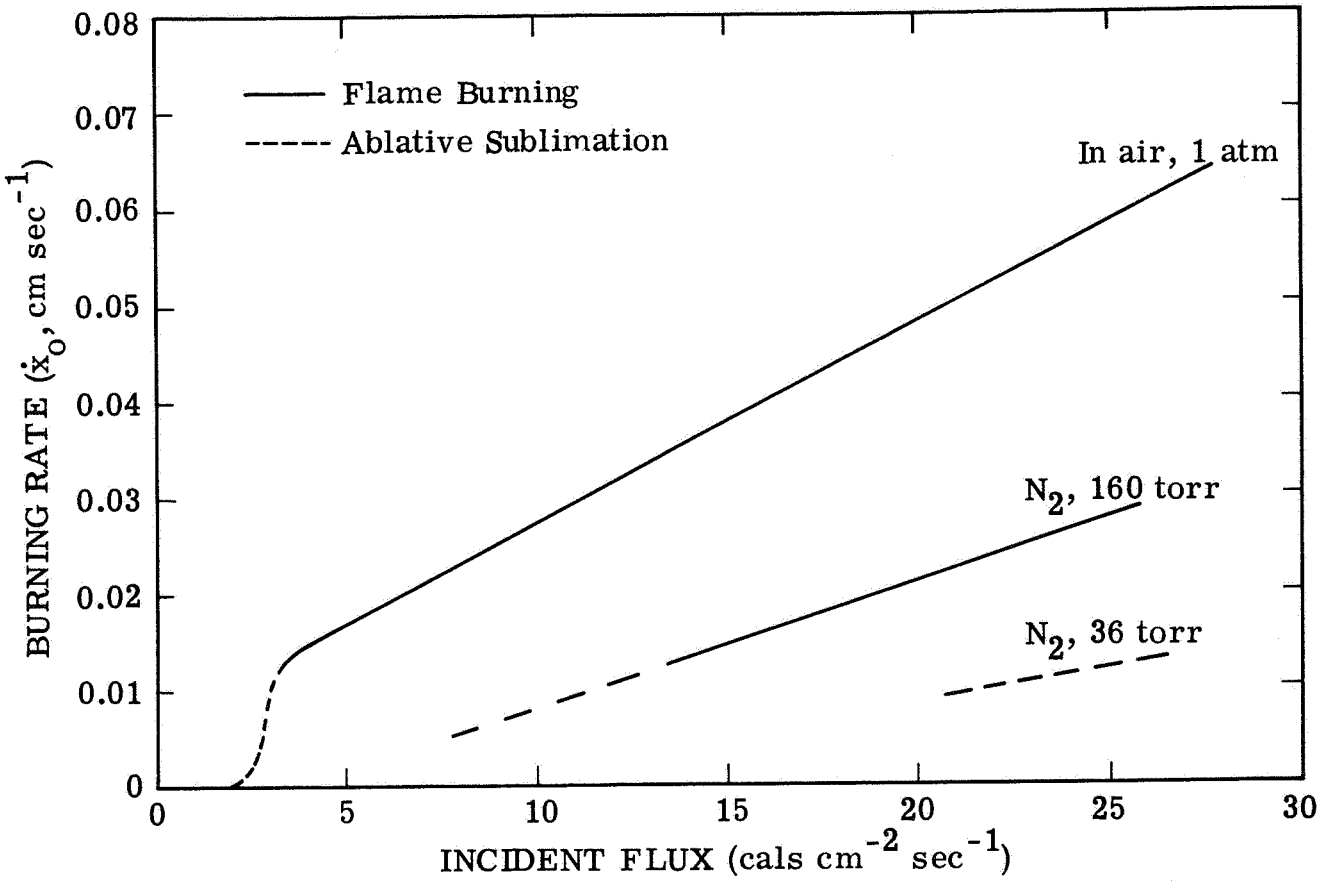

Figure 6. Laser-Induced Combustion of Ammonium Perchlorate.

conclusions can be drawn. At a high constant flux of 23 cals cm^{-2} sec^{-1}, the transition from ablative sublimation to flame-burning occurs near 100 torr. At lower fluxes of the order of 10 - 15 cals cm^{-2} sec^{-1}, the transition occurs near 160 torr. The transition occurs near 760 torr at still lower fluxes of the order of 2 - 3 cals cm^{-2} sec^{-1}. Fluxes in excess of 28 cals cm^{-2} sec^{-1} would be required in order to induce flame burning at pressures of the order of 36 torr. These tentative estimates of threshold pressure vs. threshold ignition flux are plotted in Figure 7.

4. Chemical Composition

The results of several composition measurements of the laser-induced ammonium perchlorate flame are shown in Table I. The data at 10, 19, 30 and 63 torr were obtained at high laser power levels [~23 cals cm^{-2} sec^{-1}], while the data at 760 torr were obtained at lower laser power levels [~13 cals cm^{-2} sec^{-1}].

As indicated in footnote (a), the data are not corrected for the preferential absorption of the highly polar gases HCl and H_2O on the walls of the probe. Accordingly, the data show H- and Cl-atom balances that are invariably lower than the theoretical values 40% and 10% respectively. The N atom balance is invariably larger than the theoretical 10% value. The O atom balance is usually close to the theoretical 40% value since it is present in H_2O which is strongly absorbed, and also in NO and O_2 which are not as strongly absorbed. The absorption effects thus tend to cancel for the O-atom balance.

The data at 10 torr are averages for two samples: one consisting of pure AP, the other containing a thin 10 mil film of polystyrene near the center of the sample. The two runs were in good agreement indicating that in these runs the probe was sampling essentially the pure AP flame. It is interesting to note that for the low-pressure pure AP sample, the decomposition products were observed even though there was not enough visible luminosity to clearly indicate the presence of a decomposition flame.

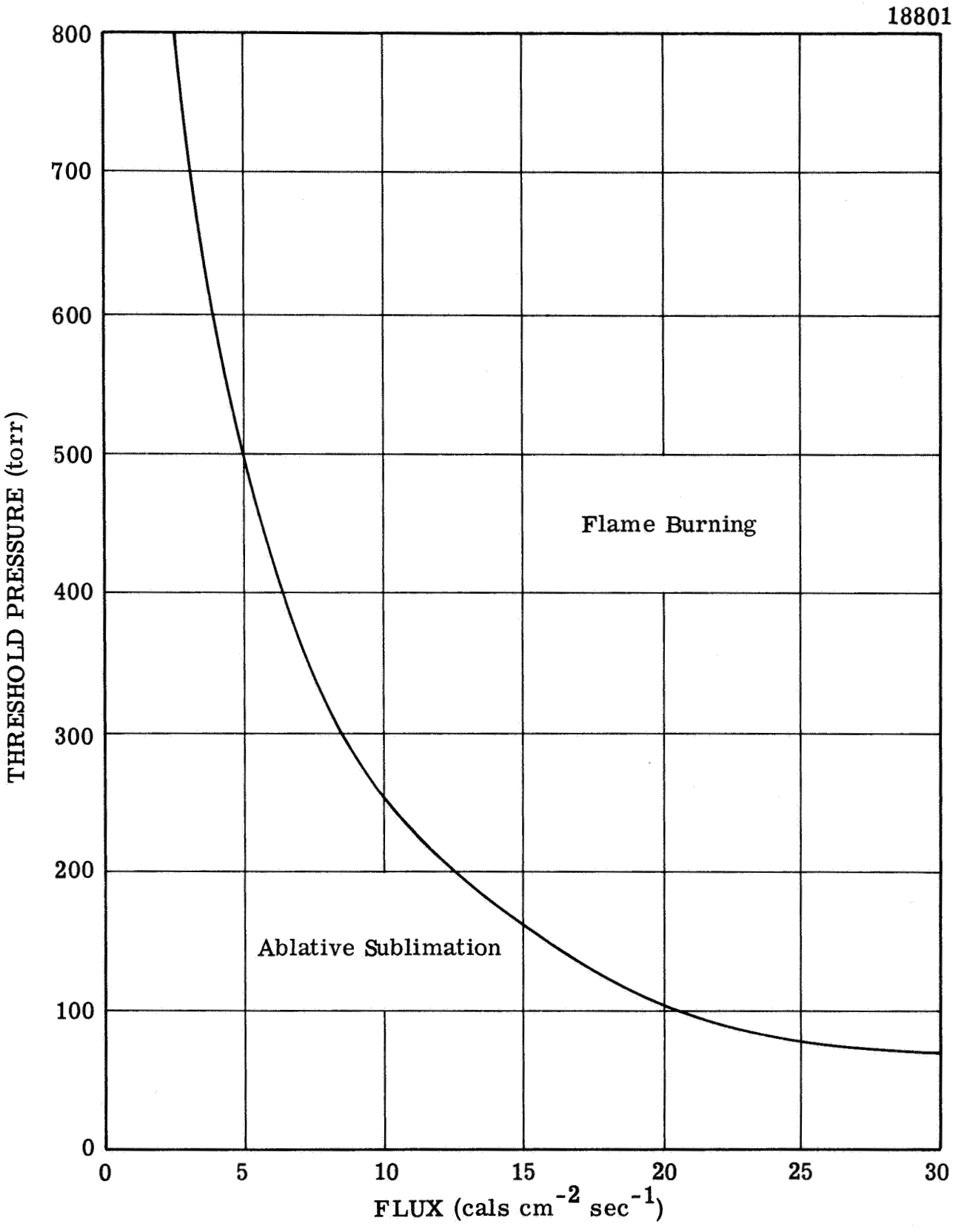

Figure 7. Ignition Flux Versus Pressure (For Transition from Ablative Sublimation to Flame-Burning).

Table I. Chemical Composition of Laser-Induced Pure AP Flame[a,b]

Percent of Total

Product	Background Pressure (Argon), Torr				
	10	19	30[c]	63	760 (in air)
H_2O	6	29	37	58	25
N_2	25	12	14	8	11
NO	12	15	15	12	25
O_2	52	36	25	15	30
HCl	2	5	6	6	7
N_2O	1	1	2	1	2
NO_2	2	2	1	-	1

[a]These data are not corrected for the preferential wall absorption of the polar constituents HCl and H_2O. They are also uncorrected for a small transmission ratio which tends to reduce the sensitivity of the instrument to the heavier masses.

[b]These data are corrected for the relative ionization efficiency of the molecular products at the 80-90 eV electron energy used in these experiments.

[c]These data (at 30 torr) were obtained from a composite sandwich of polystyrene-perchlorate rather than for pure AP; however, so little polystyrene was present that the products analyzed were mainly from the pure AP flame.

The data tend to show an apparent increase in relative H_2O abundance with increasing pressure, and a decrease in O_2 abundance with increasing pressure. It is difficult to say that this effect is truly representative of the flame composition. It could be caused by a reduced sensitivity to H_2O at the lower pressures caused by wall absorption effects. These data were obtained with a convoluted, flexible, stainless-steel side-arm between the probe and the spectrometer. Absorption effects were quite marked. This side-arm was subsequently replaced with a Teflon tube with which the composite composition traverse measurements described in Section III B were obtained. Some of the composite data may be representative of the pure AP flame, and will be discussed in III B.

B. BINDER-PERCHLORATE SANDWICH COMPOSITES

1. Fuel Polymers

Infrared absorption measurements were made for pure AP and a wide variety of polymeric binders. The AP absorption data were in substantial agreement with previous measurements reported in the literature. The optical absorption depth for pure AP was of the order of 40μ for radiation of 10.6μ wavelength. The various organic polymers exhibited a wide variety of absorptivities to the laser wavelength. The condition required for a laser source to be a good simulation of a thermal-conductive flame-source is that the optical absorption depth in the polymer be negligibly small compared with the preheat zone thickness in the solid. The absorption measurements indicate that this condition is satisfied for pure AP and most of the polymeric materials of interest.

A practical problem has existed in the laser-assisted sandwich combustion; namely, getting the sample to burn with a flat surface. The regressing face has usually been an irregular, inverted-wedge type surface, and this has been determined to be due to three causes: (1) non-uniform radiant flux over the cross-sectional area of the laser beam; (2) possible heat feedback from the gas flame, which, if occurring at low pressure, would be of different magnitude at various regions over the sandwich surface; and (3) different rates of ablation of AP and binder. Items (1) and (2) are discussed elsewhere in this report. In this section brief mention will be made of some qualitative tests and observations on the pyrolysis of polymers in the laser which relate to item (3).

At 0.1 atm pressure and with a laser flux of a few cal/cm^{2}sec, the burning rate of AP is approximately 0.1 mm/sec. For sandwich configurations it is desirable to have a polymer that ablates at approximately the same rate under the same conditions. We have pyrolyzed specimens of several types of polymers over a range of fluxes and in an N_2 atmosphere. Observations were made from motion pictures which were taken. The materials selected were polystyrene, polyvinyl chloride, polymethyl methacrylate, and carboxy-terminated polybutadiene. The relative extents and rates of melting, charring and gasification were observed. PMM was found to be the most ideal choice for sandwich-type propellant samples. PVC and CTPB were satisfactory also, but polystyrene was found to melt too readily and gasify too rapidly. Accordingly, PMM was selected for most of the sandwich burning experiments.

Measurements were made of the composition of the laser-induced pyrolysis products of two of these polymers. Typical results for polystyrene are shown in Figure 8. Data obtained for PMM have not yet been analyzed.

2. Gas Flow Patterns

The technique of incorporating particles into the propellant sandwiches to determine the aerodynamic structure of the flame is valid only if the particles follow the gas stream with reasonable accuracy. A particle starts at rest at the surface of the propellant and what one needs to know is: What size particle is necessary in order to accelerate to within a specified fraction of the gas velocity in a given distance? This size can be estimated as follows. After a particle leaves the surface it is accelerated by the flame-gas drag-force, and this acceleration force is balanced by the particle's inertia. The drag force is given by Stoke's law

$$F_{drag} = 6\pi\eta\, \Delta v\, \bar{r} \qquad (5)$$

where η is the gas viscosity, Δv is the slippage which is the difference between the gas velocity and the particle velocity, v_p, and $\bar{r}$ is the particle radius. The drag force can be equated to the acceleration force, ma, with m, the particle mass, equal to $4/3\pi\bar{r}^3\ \rho$(ρ = particle density). Solving for $\bar{r}$:

18800

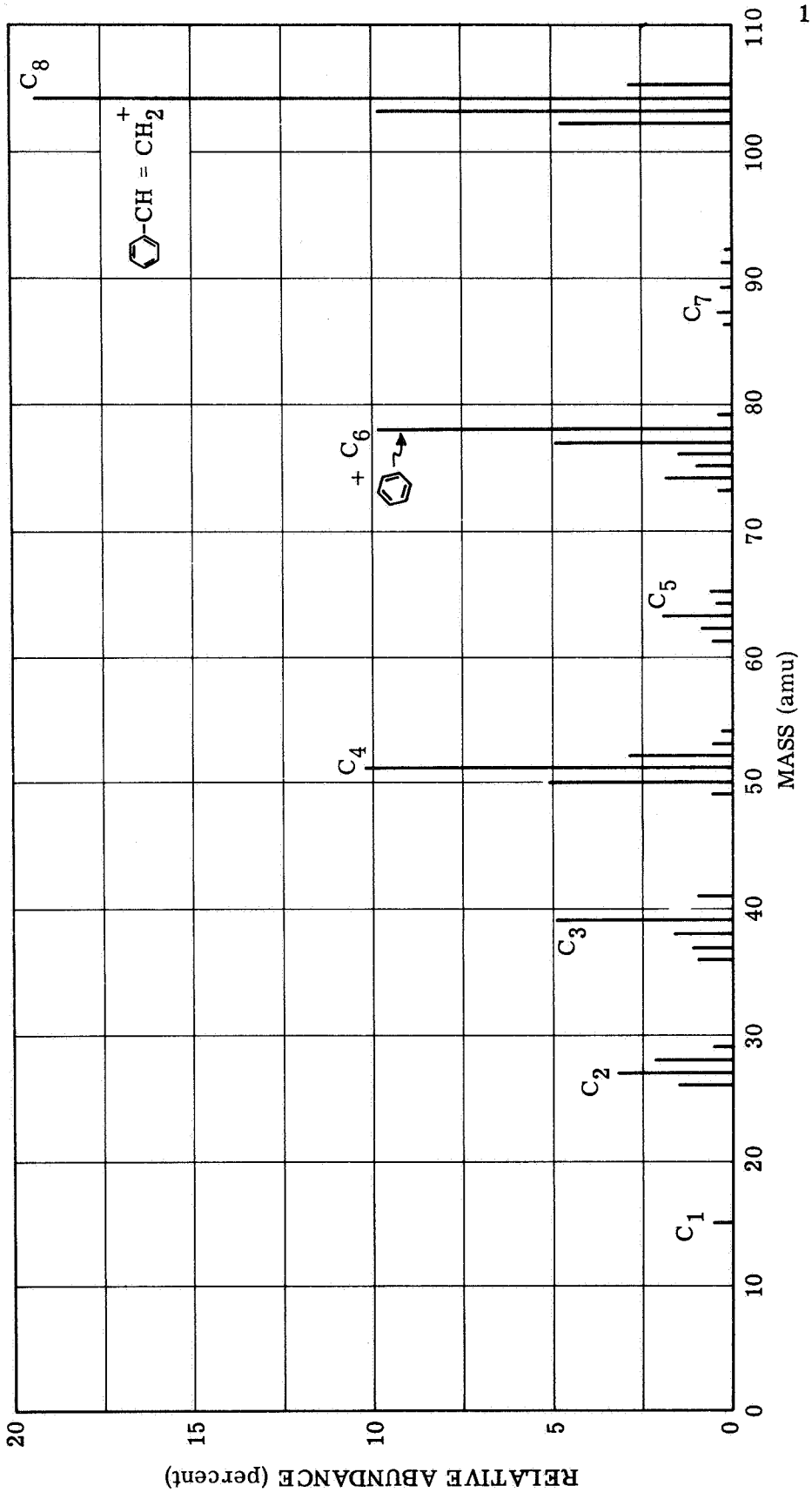

Figure 8. Mass Spectrum of Laser-Induced Pyrolysis Products of Polystyrene.
Argon Background (9 torr); Laser Flux: 26 cals cm^{-2} sec^{-1};
Electron Energy: 80 eV.

$$\bar{r} = \sqrt{\frac{18\ \eta\ v_p}{4\ a\ \rho}} \qquad (6)$$

Estimating η as 5×10^{-4} g/cm sec and ρ as 4.0 g/cc for Al_2O_3; writing the average acceleration, $\underline{a}$, as the gas velocity divided by the residence time, v_g/τ; and requiring a slippage of 20 percent, i.e., $v_p = 0.8\ v_g$, $\Delta v = 0.2\ v_g$,

$$\bar{r} = \sqrt{\frac{9.0 \times 10^{-4} \times 0.2\ v_g}{4(v_g/\tau)\ \ 4.0}} = \sqrt{1.1 \times 10^{-4}\ \tau}\ \text{cm} . \qquad (7)$$

We can compute a value for τ by dividing the flame zone thickness by v_g. The zone thickness we take as 0.2 cm. v_g is given by $v_g = \dot{x}_o\ \rho_s/\rho_g$ where $\dot{x}_o$ is the linear regression rate of the sandwich, ~0.03 cm/sec; ρ_s its density, ~2 g/cc; and ρ_g the gas density, a reasonable average value for which is 2×10^{-5} g/cc based on a pressure of 0.1 atm, an average molecular weight of 30, and an average temperature of 1500°K. Hence, τ is 7×10^{-5} sec, and $\bar{r}$ becomes approximately 1 micron. Such calculations provide a basis for determining roughly the size of the particles to use. The actual particles in the flow pattern experiments were of 2-5 microns in radius, chosen to satisfy the above calculations and also the requirement that they be large enough to reflect or scatter enough light to see them.

Approximately 35 runs were carried out to study the gas flow patterns. It was anticipated that particle tracks similar to those photographed for gas flames would be obtained (2,3). In fact, quite different results were found which we do not as yet completely understand. Instead of observing distinct particle tracks originating from the point at the binder-AP interface where the Al_2O_3 was located, sporadic streaks were observed. These would originate from any random point on the entire sandwich surface. In Figure 9 we show a somewhat idealized line-drawing of what a deflagrating propellant sandwich looks like. There are three flame zones, the two orange zones being the AP decomposition flame and the blue zone the fuel binder-oxidizer flame.

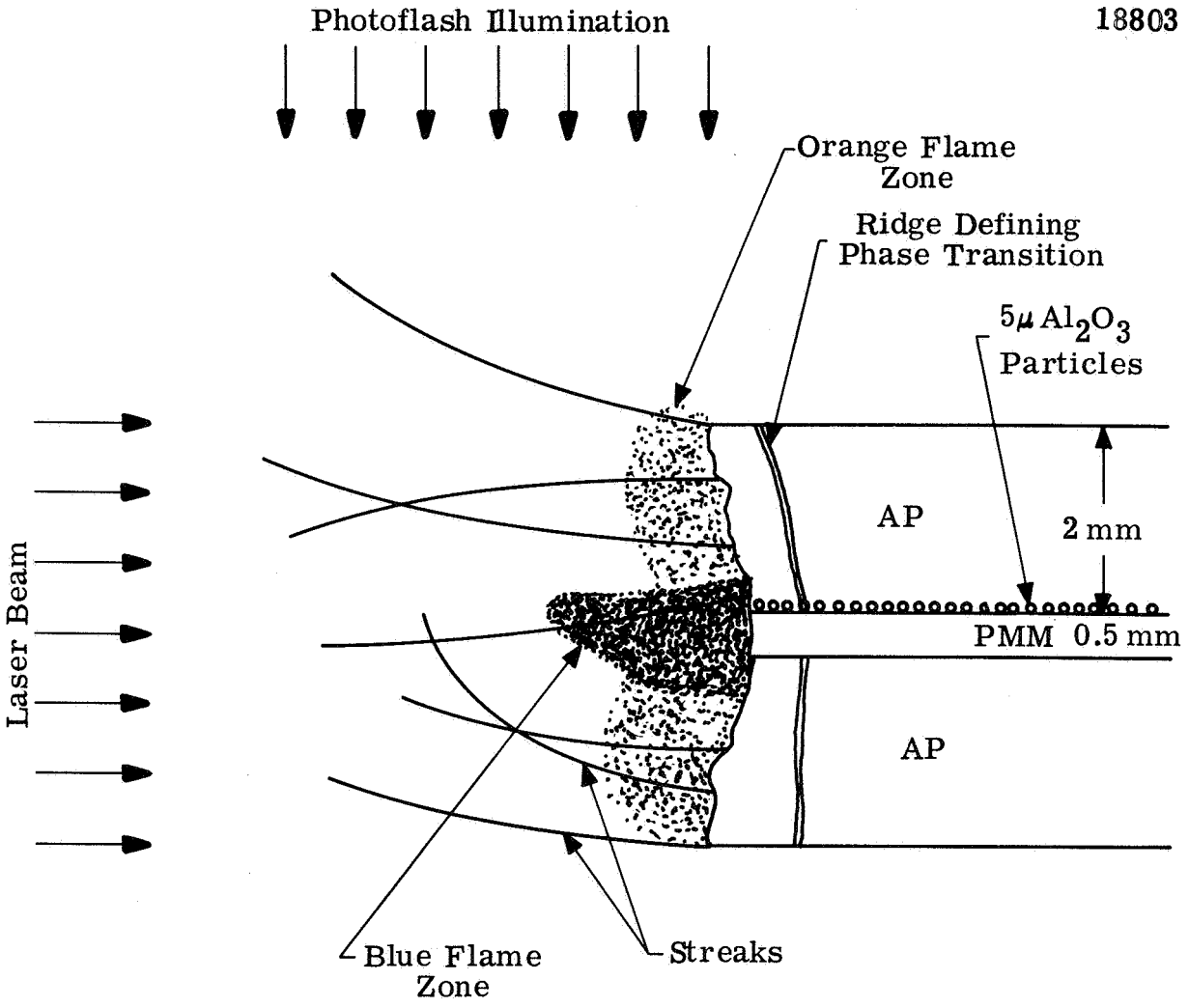

Figure 9. Diagram of Burning Propellant Sandwich at 0.1 atm Illustrating Flame Zones and Particle Streaks.

The drawing is approximately to scale. The ridge defining the AP phase-transition is discussed in a later section. The streaks that are illustrated through the flame and post-flame gases are observed only when particles are incorporated in the sandwich. A number of streaks as shown in the figure would not all appear at one time, but rather one or sometimes two tracks would appear at intervals of a few tenths of a second. The paths of the tracks would curve up or down and sometimes were very erratic.

At present we believe the streaks are caused by the Al_2O_3 particles migrating over the surface of the propellant. The tracks may be agglomerations of particles or, more likely, small fragments of AP which are somehow dislodged and shoot out from the surface. It is certain that the tracks are not following the flow because it was possible to measure velocity in one photograph and this was substantially lower than the calculated gas velocity. It is noted that the idea of Al_2O_3 migrating over the propellant surface is not inconsistent with a finding of Hightower and Price (5). In sandwich burning experiments at high pressure and using single crystals of AP, they found that the AP surface of quenched samples was markedly changed when lithium fluoride was incorporated into the binder. Experiments are planned to pursue the curious behavior observed in these flow pattern measurements.

3. General Remarks on Flame Characteristics

It is of interest to specify approximately the conditions under which sandwich propellants will exhibit premixed or diffusion flames. Consider a 0.1 atm flame with polymer slab thicknesses of, say, 50, 500 and 5000 microns. We can calculate corresponding "characteristic diffusion times," t_d, from the equation, $t_d = x^2/2D$, where x is given by the thicknesses above and D is the diffusion coefficient. A reasonable value for the latter at 0.1 atm and 1500°K is 20 cm^2/sec. The values of t_d then are roughly 10^{-6}, 10^{-4} and 10^{-2} seconds, respectively. (The last value is somewhat fictitious since the AP slabs are thinner than the assumed binder).

These values can be compared with the residence time for an element of reactant in the flame zone. This will be the τ which was previously estimated in Section III, B,2 as of the order of 10^{-4} seconds. Thus it appears that for a binder thickness of 0.5 mm, which was most commonly used in this study, the characteristic diffusion time and residence time are comparable. The flame is then expected to be neither purely premixed nor diffusion. The flame for which the composition traverse is shown in Figure 11 should be essentially a diffusion flame according to this analysis.

Next we can consider what is called in Figure 9 the ridge defining the phase transition. The orthorhombic to cubic phase transition which AP undergoes at 243°C has been used by others (6) as a temperature marker in the combustion wave from which the surface temperature of AP could be calculated. On motion pictures of the deflagrating sandwiches, we have consistently noticed a line or ridge a short distance from the AP surface which regresses with the surface. We suspect this to be the phase transition boundary, and to provide one check on this assumption we have made the following simple calculation. The boundary lies roughly 1 mm below the AP surface. Assuming a surface temperature 300 degrees above the phase transition temperature and a linear gradient in the solid, $\Delta T/\Delta x$ is ~3000 deg/cm. The thermal conductivity of AP is ~0.001 cal/cm sec degrees, hence the heat flux into the solid ~3 cal/cm^{2}sec. The flux from the gas must therefore be of the order of 10 cal/cm^{2}sec, since it must provide an additional vaporization heat which is probably somewhat higher. Since this is close to the estimated heat flux from the laser plus the gas flame, the assumption that we are seeing the phase-transition boundary in the combustion is well supported.

4. Temperature Profile

Several temperature traverses were made of sandwiches consisting of 0.020" PMM and AP. The results of these measurements are shown in Figure 10. A decomposition flame was clearly present in the runs at 80 torr. The temperature profiles indicate that the conductive heat flux from the flame to the surface is of the order of 0.9 to 1.3 cals cm^{-2} sec^{-1} at this pressure. This

heat flux is from 7 to 15% of the magnitude of the incident radiant flux. The observed surface temperatures are in the range 690-780°K, in excellent agreement with the measurements of previous investigators (7).

The low-pressure run at 0 - 3 torr indicates a negligible heat-release in the gas phase, and its subsurface temperature profile is essentially identical with the profiles of the higher pressure runs. It is clearly maintained entirely by the external laser source.

At 80 torr, the flame zone thickness is of the order of 0.14 cm, which is still somewhat smaller than is desirable for good spatial resolution. Since the flame zone thickness is essentially infinite for the 0 - 3 torr run, a convenient operating pressure in the range 10 - 50 torr should be optimum for studying the structure of the fuel-perchlorate diffusion flame.

The observed flame temperature of 1900-2000°K is intermediate between the temperature of pure AP (~1200°K) and that of a propellant mixture (~2700°K). This is in good agreement with theoretical expectations for the diffusion flame.

5. Composition Measurements

A series of composition traverses were made of AP-PMM sandwiches at pressures of 40, 60 and 30 torr. The best measurements from a total of four traverses through a composite sample are shown in Figure 11. The probe was initially 1-2 mm above the surface, and was made to traverse across the surface by pivoting the probe about an axis above the sample. The probe was initially near the edge of the sample as indicated in the figure. The peak at mass 40 is due to the Argon gas background. The peak at mass 28 is the sum of contributions from N_2, CO and possibly C_2H_4. The nitrogen is from the AP; the CO can come either from the PMM, or as a decomposition product of the diffusion flame. The mass 30 and 32 peaks are from NO and O_2 and are clearly from the AP flame. The mass 18 peak is from H_2O which is a product of both the pure AP flame and the diffusion flame. The peak at mass 26 is from C_2H_2; while the peak at 12 is C^+, dissociatively ionized from various hydrocarbons and/or oxides

Run No.	Pressure (torr)	Laser Flux (cals $cm^{-2} sec^{-1}$)	Burning Rate ($\dot{x}_o$, cm sec^{-1})	Conductive Heat-to-Surface $\lambda g(\frac{\partial T}{\partial x})_{S_g}$, (cals $cm^{-2} sec^{-1}$)
1	80	Sample Poorly Aligned		0.9
2	80	14	0.04	1.1
3	80	7	0.02	1.3
4	0-3	12	0.02	< 0.1

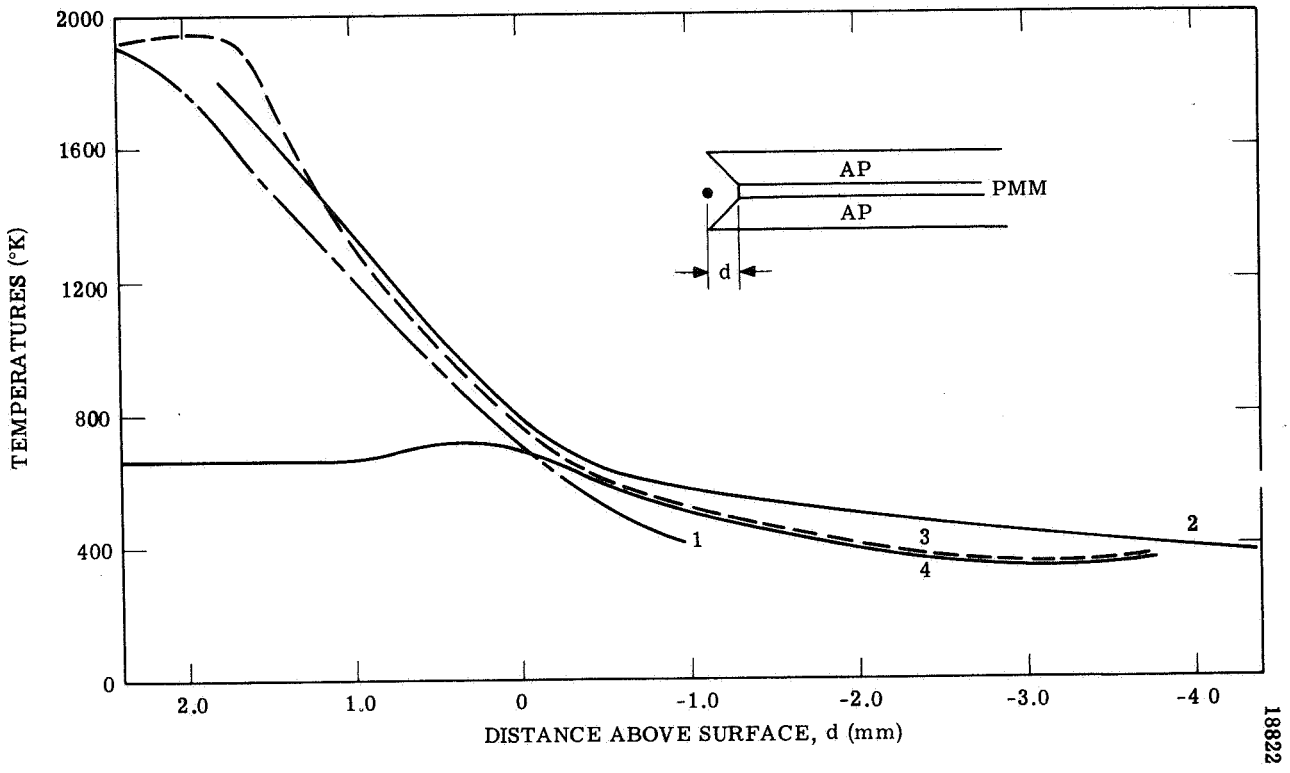

Figure 10. Temperature Profiles for AP-PMM (20 mil) Composites.

18804

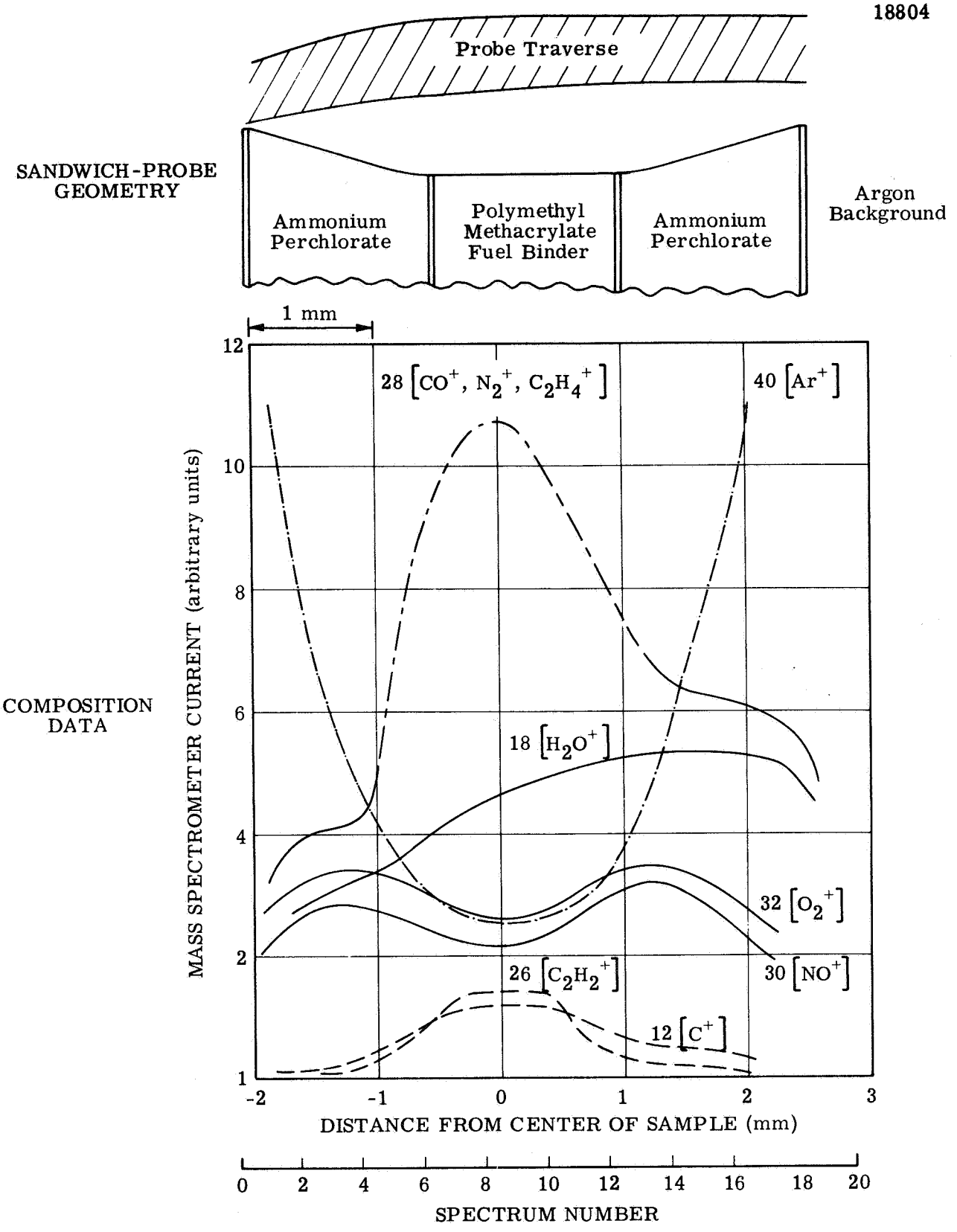

Figure 11. Composition of Laser-Induced, Composite-Sandwich Flame. Chamber Pressure: 60 torr (Argon), Spectrometer Pressure: 8×10^{-5} torr; Laser Flux: 10 cals cm^{-2} sec^{-1}; Electron Energy: 54 eV.

of carbon. These results are excellent confirmation of the existence of two distinct zones: a zone containing the pure AP flame and a zone containing the pyrolysis products of PMM. The minimum in the O_2 and NO peaks at the center of the sample is caused by the fact that the pure AP flame tends to be excluded from the region above the binder by the decomposition products of the binder. The peak in the $C_2H_2^+$ intensity near the center of the sample is caused by the unreacted decompositon products of the PMM. The shape of the mass 28 peak clearly indicates that it is a superposition of N_2 from the pure AP flame, and CO which can come from either the AP-binder diffusion flame, or the binder pyrolysis. The marked skewness in the H_2O peak is caused by wall absorption effects previously discussed. A similar skewness is observed for the HCl peak (not shown in the figure).

The choice of PMM as a binder introduces several ambiguities in the spectral identification. The ambiguity between N_2 and CO can be avoided by using $N^{15}H_4\ ClO_4$. The N_2 is a product of the pure AP flame, while the CO is a product of the composite flame. The use of an oxygen-containing binder such as PMM introduces still another ambiguity between the binder pyrolysis products (CO, CO_2) and the same products formed in the composite flame. The H_2O observed is formed mainly from two sources: AP flame or composite diffusion-flame. It would be deisrable to choose a binder material which had similar pyrolysis rate to PMM, but whose composition were such that these ambiguities were minimized or eliminated.

If one uses the composition data near the edge of the sample as being representative of the composition of the pure AP flame, one obtains fair agreement with the previous measurements in Table I: H_2O (42%), N_2 (26%), NO (9%), O_2 (11%), HCl (8%), N_2O (3%), NO_2 (1%), and some chlorine.

IV. FUTURE PLANS

The experimental capability of obtaining measurements of the temperature, composition and flow fields of laser-induced, low pressure diffusion flames of ammonium perchlorate and organic binders will be utilized for a systematic and accurate acquisition of these data. Composition, temperature and flow structure will be determined as a function of pressure and radiant flux, in the pressure range 0.005 to 0.25 atm, and in the laser-flux range 1-15 cals cm^{-2} sec^{-1}. The data so obtained will be analyzed as required for extrapolation to the higher pressure ranges and smaller dimensions of flames in ordinary combustion environments.

Although the apparatus developed during the first year of this program is clearly adequate for accomplishing the objectives of determining the temperature and composition fields, nevertheless there are several problem areas that indicate that refinements of the experimental apparatus are desirable. These are:

(1) Improvement of the spatial uniformity and temporal stability of the radiant laser source.

(2) Redesign of the probe positioning system to permit more precise control of the probe location relative to the solid surface during traverses.

(3) Addition of a thermocouple to the quartz probe to permit the simultaneous detection of both the temperature and composition fields.

(4) Modification of the probe side-arm to reduce still further absorption effects and time delays.

(5) Improvement of the external source of illumination and photographic methods to provide for accurate measurements of the flow field.

It is planned to develop these improvements as an integral part of the program of data acquisition.

V. REFERENCES

1. Friedman, R., Nugent, R. G., Rumbel, K. E., and Scurlock, A. C., Sixth Symposium (International) on Combustion, p. 612, Reinhold Publishing Corporation, New York, 1957.

2. Lewis, B., and von Elbe, G., Combustion, Flames and Explosions of Gases, 2nd Edition, Academic Press Inc., New York, N. Y., 1961.

3. Fristrom, R. M. and Westenberg, A. A., Flame Structure, McGraw-Hill Book Co., New York, N. Y., 1965.

4. Hertzberg, M., "The Laminar Premixed Combustion of Composite Propellants". Unpublished.

5. Hightower, J. D. and Price, E. W., "Two-Dimensional Experimental Studies of the Combustion Zone of Composite Propellants," ICRPG 2nd Combustion Conference, Vol. I, p. 421, May 1966.

6. Beckstead, M. W. and Hightower, J. D., "On the Surface Temperature of Deflagrating Ammonium Perchlorate Crystals," AIAA Paper 67-68, Jan. 1967.

7. Powling, J., "Experiments Relating to the Combustion of Ammonium Perchlorate-Based Propellants," 11th Combustion Symposium (1967), p. 447.

8. von Elbe, G. et al., "Chemical Kinetic and Physical Processes in Composite Solid-Propellant Combustion", ARC Report NAS 1-6440 January 1967.

VI. NOMENCLATURE

$(Cg)_g$, $(Cg)_X$, $(Cg)_A$, $(Cg)_B$	Heat capacities per gram of the gas above the surface (g), the solid (X), the reactant(s) (A), the product(s) (B) [cal gm^{-1}].
D	The mutual interdiffusion coefficient for fuel and oxidizer gases [cm^2 sec^{-1}].
ε_s	The emissivity of the propellant surface [dimensionless].
ΔH_g	The latent heat of vaporization per gram of solid [cals gm^{-1}].
$i(T,\alpha,\lambda)$	The burning-rate dependent factor for the non-adiabatic conductive-convective losses [cals cm^{-3}].
$(I_L)_S$	The total non-adiabatic losses from the surface-state zone (S) to the surroundings [cals cm^{-2} sec^{-1}].
$(I_L)_o$	The burning-rate independent loss term [cals cm^{-2} sec^{-1}].
$(I_R)_o$	The net radiant flux loss from the surface to the surroundings [cals cm^{-2} sec^{-1}].
I	The incident radiant flux [cals cm^{-2} sec^{-1}].
r	The surface reflectivity (dimensionless).
$\bar{r}$	The average particle radius [cm].
ρ_x and ρ_g	The density of the solid and the gas [gms cm^{-3}].
T	The temperature [°K].
$\bar{T}_s$	The surface temperature [°K].
T_b	The temperature of the burned gases [°K].
T_p	An equivalent "preheat" temperature [°K].
T_u	The initial temperature of the unburned solid [°K].
v_g	The linear velocity of the gas above the burning surface [cm sec^{-1}].

$v_{A \to B}$	The burning velocity of a simulated flame above the surface, preheated to the surface temperature [cm sec^{-1}].
Δv	The difference between the gas velocity and particle velocity [cm sec^{-1}].
x	The linear coordinate [cm].
x_o	The planar surface discontinuity [cm].
$\dot{x}_o$	The velocity of the preferred coordinate frame (the laminar burning rate) [cm sec^{-1}].
η	The gas viscosity [gm cm^{-1} sec^{-1}].

VII. ACKNOWLEDGMENTS

The authors are indebted to several of the scientists of the Langley Research Center for their helpful advice and assistance during the performance of the contract. These include: Dr. A. Saunders, who was project monitor during the initial phase of the contract, Mr. H. J. Hale, the present project monitor, and Dr. G. L. Pellett.

The authors wish also to express their appreciation to Messrs. Richard Lee and Scott Gosnell of Atlantic Research Corporation for their helpful assistance in the design, construction and operation of the experimental apparatus.